Doklady Physics, Vol. 47, No. 3, 2002, pp. 233–237. Translated from Doklady Akademii Nauk, Vol. 383, No. 1, 2002, pp. 61–66.

MECHANICS

New Stationary Solutions to the Problem of Three Vortices in a Two-Layer Fluid

M. A. Sokolovskiĭ* and J. Verron**

Presented by Academician V.V. Kozlov September 4, 2001

Received September 6, 2001

1. The universally integrable problem of three vortices [1, 4–6] has attracted the interest of researchers for over one hundred years [6]. This is not associated only with the vortex problem in itself but also has numerous analogies in the mechanics of solids, astrophysics, the dynamics of superfluid helium, and mathematical biology [1, 5]. A new peak of interest in this problem was stimulated by the discovery of so-called three-polar structures [13], i.e., symmetric triples of vortices ($-\kappa$, 2κ, $-\kappa$) and by later observation of their spontaneous origin from chaos [12]. In most studies [1, 4–7, 10, 12–15], the dynamics of vortices was analyzed in the framework of the homogeneous-fluid model. At the same time, the geophysical problems (some of them were discussed in [2, 3, 8, 11]) are characterized by noticeable density stratification. In this paper, we analyze the problem of three vortices that exist in a two-layer fluid and have zero total intensity.

2. We take the following assumptions: (i) the upper and lower layers have equal thickness values ($h_1 = h_2 = 1/2$) and the densities ρ_1 and ρ_2 in the layers satisfy the condition $\Delta\rho = \rho_2 - \rho_1 > 0$; and (ii) one vortex with an intensity κ_1^1 corresponds to the upper layer, whereas two vortices with intensities κ_2^1 and κ_2^2 are located in the lower layer. The complex form of equations of motion for three discrete vortices in two immiscible fluid layers rotating with a constant angular velocity (in the presence of a hard cap on the upper surface) is

$$\frac{d\overline{z_1^1}}{dt} = \frac{1}{2\pi i}\sum_{j=1}^{2}\frac{\kappa_2^j}{z_2^j - z_1^1}\left[1-\gamma\left|z_2^j - z_1^1\right|K_1\left(\gamma\left|z_2^j - z_1^1\right|\right)\right], \quad (1)$$

$$\frac{d\overline{z_2^m}}{dt} = \frac{1}{2\pi i}\left\{\frac{\kappa_1^1}{z_1^1 - z_2^m}\left[1-\gamma\left|z_1^1 - z_2^m\right|K_1\left(\gamma\left|z_1^1 - z_2^m\right|\right)\right]\right.$$
$$\left. + \frac{\kappa_2^{3-m}}{z_2^{3-m} - z_2^m}\left[1+\gamma\left|z_2^{3-m} - z_2^m\right|K_1\left(\gamma\left|z_2^{3-m} - z_2^m\right|\right)\right]\right\}. \quad (2)$$

Here, $z_n^m = x_n^m + iy_n^m$ is the complex coordinate of the mth vortex in the nth layer; the overbar implies complex conjugation; the parameter γ is inversely proportional to the Rossby internal deformation radius

$$\lambda = \left[\frac{g\Delta\rho h_1 h_2}{\rho_0 f^2(h_1+h_2)}\right]^{1/2};$$

K_k is the kth-order modified Bessel function of the second kind; g is the acceleration of gravity; and f is the Coriolis parameter equal to the double angular velocity of the fluid-plane rotation about a normal to this plane. According to assumption (ii) above, the variable m in Eq. (2) takes the values 1 and 2. Thus, Eqs. (1), (2) are the set of ordinary differential equations that should be complemented by initial conditions for the original coordinates of all three vortices.

The set of Eqs. (1), (2) can be represented in the standard Hamiltonian form with the Hamiltonian

$$H = -\frac{1}{2\pi}\{\kappa_2^2\kappa_2^1[\ln d_{22}^{12} - K_0(\gamma d_{22}^{12})]$$
$$+ \kappa_1^1\kappa_2^1[\ln d_{21}^{11} + K_0(\gamma d_{21}^{11})] + \kappa_1^1\kappa_2^2[\ln d_{21}^{21} + K_0(\gamma d_{21}^{21})]\}, \quad (3)$$

where $d_{kl}^{mn} = |z_l^n - z_k^m|$. In addition to Hamiltonian (3), the original set has the first integrals for the momenta

$$P = \kappa_1^1 z_1^1 + \kappa_2^1 z_2^1 + \kappa_2^2 z_2^2, \quad \bar{P} = \kappa_1^1 \bar{z}_1^1 + \kappa_2^1 \bar{z}_2^1 + \kappa_2^2 \bar{z}_2^2$$

and the angular momentum

$$M = \kappa_1^1|z_1^1|^2 + \kappa_2^1|z_2^1|^2 + \kappa_2^2|z_2^2|^2,$$

whose values are evidently determined by the initial conditions.

* *Water Problems Institute, Russian Academy of Sciences, Novaya Basmannaya ul. 10, Moscow, 107078 Russia*
E-mail: m_sokolovskiy@mail.ru

** *Laboratoire de Geophysique et Industriel Courants, Centre National de la Recherche Scientifique, Grenoble, France*
E-mail: verron@hmg.inpg.fr

1028-3358/02/4703-0233$22.00 © 2002 MAIK “Nauka/Interperiodica”

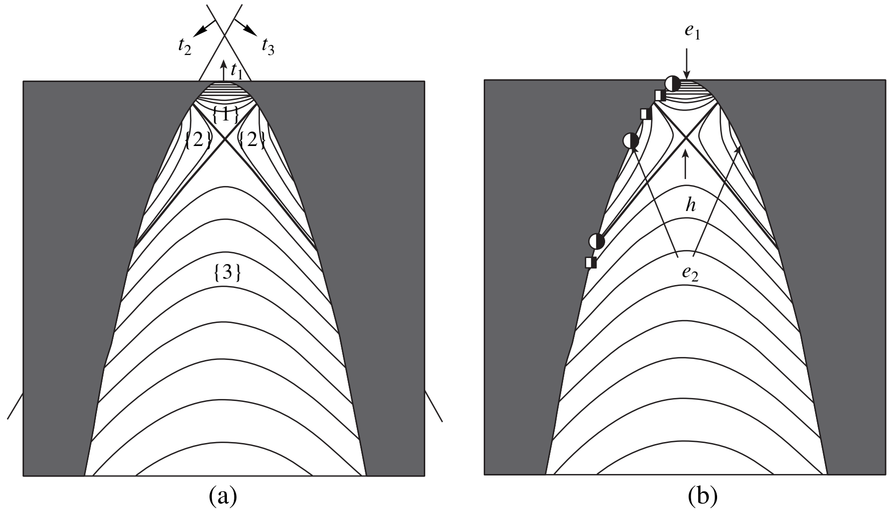

Fig. 1. (a) Phase portrait of the relative motion for a three-vortex system in a two-layer fluid under conditions (4) and $P = 1.7$. Thick lines are separatrices that separate the regions of different types {1}, {2}, and {3} of interactions between the vortices. The dark region is the nonphysical region of the phase plane (axes of trilinear coordinates are also shown). (b) The same as in Fig. 1a with the singular points indicated. Squares and circles on the boundary of the physical region correspond to the coordinates of the representation points in the phase space for the original configurations of the vortices in the numerical calculations presented in Figs. 2 and 3, respectively.

It is easy to verify that the invariants H, M, and $P \cdot \bar{P}$ are in involution, and therefore set (1), (2) always has a regular solution [1, 4].

In what follows, we assume that the total intensity of vortices is zero and

$$\kappa_1^1 = -2\kappa, \quad \kappa_2^1 = \kappa_2^2 = \kappa > 0. \tag{4}$$

Thus, the upper-layer vortex is attributed to the anticyclonic vorticity compensated by the two cyclones in the lower layer.

3. We now assume that $P \neq 0$. In this case, the relative motion can be analyzed in the trilinear coordinates [1, 7, 15]

$$t_1 = -\frac{3\kappa_2^1\kappa_2^2(d_{22}^{21})^2}{P^2}, \quad t_2 = -\frac{3\kappa_1^1\kappa_2^2(d_{21}^{21})^2}{P^2},$$

$$t_3 = -\frac{3\kappa_1^1\kappa_2^1(d_{21}^{11})^2}{P^2},$$

which possess the obvious property

$$t_1 + t_2 + t_3 = 3.$$

In the plane specified by the coordinates t_1, t_2, t_3 (whose meaning is illustrated in Fig. 1a), it is necessary to separate so-called physical regions where the triangle inequality is satisfied. Under condition (4), this implies that

$$12t_1 + (t_2 - t_3)^2 \le 0 \quad \text{for} \quad t_1 < 0, \quad t_2 \ge 0, \quad t_3 \ge 0.$$

In the trilinear coordinates, the isolines of Hamiltonian (3) coincide with those of the function

$$W(t_1, t_2, t_3) = \ln\left[\frac{-t_1}{t_2 t_3}\right]$$

$$-2\left[K_0\left(\gamma\sqrt{\frac{-t_1P^2}{3\kappa^2}}\right) + 2K_0\left(\gamma\sqrt{\frac{t_2P^2}{6\kappa^2}}\right) + 2K_0\left(\gamma\sqrt{\frac{t_3P^2}{6\kappa^2}}\right)\right].$$

In essence, these isolines are the phase trajectories for the relative motion of the three-vortex system under consideration and are shown in Fig. 1 for $P = 1.7$.

The basic general properties of the phase curves are the following.

(I) All the phase curves start and finish at the physical-region boundary. Therefore, all relative motions of vortices are periodical, and vortices pass through two collinear positions during a period. From this, it follows that exhaustive information on possible motions of the system of vortices can be acquired from the initial condition for three vortices being located in the same straight line.

(II) Possible motions for the system of three vortices can be classified into three qualitatively different types according to the initial collinear configuration of vortices.

(III) The phase portrait can have singular points of elliptic (e) and hyperbolic (h) types (see Fig. 1b).

(IV) The phase curves are symmetric about the straight line $t_2 = t_3$, because the variables t_2 and t_3 are proportional to the distances squared between the anticyclone of the upper layer and equivalent (with each other) cyclones of the lower layer.

The phase portraits (we present here only one example for a particular value of the system momentum) provide total information on the relative motion of the system of vortices. However, it is known that this analysis does not reveal all characteristic properties of the absolute motion of vortices [5]. Below, the basic features of the vortices are analyzed on the basis of numerical calculations. We also present the trajectories of vortices, indicating (by markers) their synchronous collinear positions additionally marked by segments passing through these positions. Without loss of generality, the original positions of vortices are attributed to the x-axis. We take $\bar{x}_1^1 = \bar{x}_2^1 = 0$ (one of the lower-layer vortices is exactly under the upper-layer vortex) and $\bar{x}_2^2 \neq 0$ as the simplest (reference) original positions of the vortices x_1^1, x_2^1, and x_2^2, respectively. In this case, the momentum P of the system of vortices is completely determined by the initial vortex position $\bar{x}_2^2$. At the same time, the sets of coordinates

$$x_1^1 = \bar{x}_1^1, \quad x_2^1 = \bar{x}_2^1 - x_0, \quad x_2^2 = \bar{x}_2^2 + x_0, \qquad (5)$$

conserve the given P value for all x_0. An arbitrary set of numerical experiments with initial conditions (5) for fixed $\bar{x}_2^2$ corresponds to a specific phase portrait (e.g., that presented in Fig. 1). In what follows, we also use the notation $X_0 = \gamma x_0$ and $X_n^m = \gamma x_n^m$ along with x_0 and x_n^m.

The trajectories and vortices (for their collinear positions) are shown in Figs. 2 and 3 by solid lines and triangles for the upper-layer vortex x_1^1, by long dashes and circles for x_2^1, and by short dashes and squares for x_2^2. The size of a marker is proportional to the intensity of the corresponding vortex. We imply the upward translational motion everywhere. In figure captions, the notation $t = (t_1, t_2, t_3)$ is used.

4. Figure 2 shows characteristic examples of motions for each of three types.

For type {1} (see Fig. 2a), the interaction between the lower-layer vortices is predominant. The system of vortices moves in the direction perpendicular to the x-axis. In this case, the anticyclonic vortex of the upper layer undergoes small periodic deviations from the rectilinear motion. The lower-layer vortices revolve in the cyclonic direction around a certain center moving translationally so that the vortices change their places in the collinear positions for each half-period.

Motions of type {2} are characterized by dominating interactions between the upper-layer vortex and one of the lower-layer vortices, which was initially located closer to the upper-layer vortex.

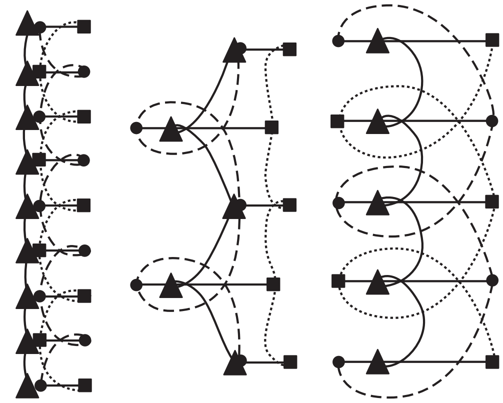

Fig. 2. Trajectories of absolute motion for $P = 1.7$. The initial conditions are specified by Eqs. (5) for $\bar{X}_1^1 = \bar{X}_2^1 = 0$; $\bar{X}_2^2 = 1.7$; $X_0 =$ (a) –0.3, (b) –0.2, (c) 1.1; and (a) $t =$ (–1.2561, 4.0692, 0.1869), (b) (–1.7543, 4.6713, 0.0830), and (c) (–15.7889, 16.2768, 2.5121).

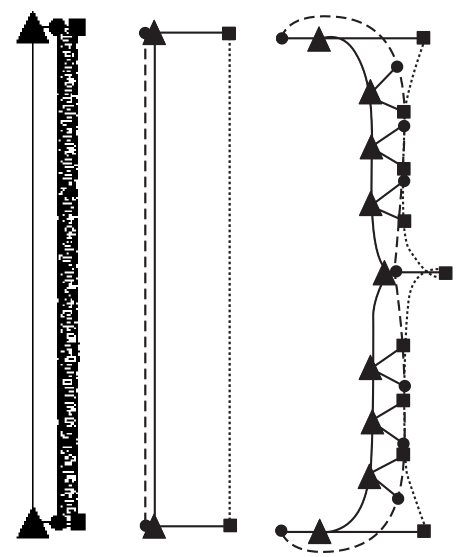

Fig. 3. The same as in Fig. 2, but for (a) $X_0 = -0.6$, (b) 0.2062, and (c) 0.9611 and (a) $t =$ (–0.2595, 2.5121, 0.7474), (b) (–4.6321, 7.5438, 0.0883), (c) (–13.6197, 14.7020, 1.9177).

According to Fig. 2c, solutions of type {3} are featured by anticyclonic revolutions of all three vortices. This is caused by the defining role of the upper-layer vortex.

The cyclicity periods for vortices in the upper and lower layers relate to each other as 1 : 2 for motions of types {1} and {3}, whereas these periods coincide in the case of type {2}. This difference is explained by the fact that each phase curve of types {1} and {3} is mirror symmetric, whereas the curve of type {2} is asymmetric.

The examples of phase curves presented in Fig. 2 correspond to the conditions when they pass far from the separatrices and singular points. However, the stationary solutions corresponding to singular points are of the most interest.

In the vicinity of the singular point e_1, the lower-layer vortices approach each other at an infinitesimal distance and should orbit a common center with a (theoretically) infinite angular velocity. In this case, interlayer interaction is manifested almost exclusively as the linear displacement of the entire configuration. In essence, the limiting-case structure is equivalent to a two-layer pair of vortices of intensities -2κ and 2κ in the upper and lower layers, respectively. The motion with characteristics close to those described above is exemplified in Fig. 3a, where $\gamma d_{22}^{12} = 0.5$ is not small. (The lower-layer vortices undergo 66 revolutions during the calculation time; to avoid overloading, we mark in the figure only the original and final collinear positions of the vortices.) With a decrease in the original distance between the lower-layer vortices, the pattern becomes less instructive. For this reason, the results of corresponding calculations are not presented.

We now consider a point e_2 belonging to the boundary of the physical region (see Fig. 1b). As is known [1], the collinear three-vortex configurations corresponding to such singular points should revolve around the vorticity center. The presence of these elliptic points under the condition of the zero total intensity of the system is a remarkable (and surprising) property of the two-layer configuration. Since, in this case, the vorticity center moves to an infinitely far point, the collinear configuration of the three vortices, as a pair of vortices, should move uniformly and rectilinearly in the direction normal to the straight line in which vortices lie (a corresponding example is shown in Fig. 3b). This configuration, naturally referred to as a triton, can be the simplest example of the vortex structures referred to as a modon with a raider [9].

A hyperbolic point h apparently corresponds to the unstable solution associated with the translationally moving configuration in the form of an isosceles triangle ($t_2 = t_3$). This configuration is illustrated in Fig. 3c exhibiting trajectories of the vortex-structure motion for which the representation point in the phase plane is originally located at the boundary of the physical region near the separatrix. The markers (positions of vortices) and segments connecting them in this figure indicate not only collinear but also other synchronous intermediate vortex configurations for time intervals during which the representation point resides in the vicinity of the intersection point h of the separatrices. These unstable configurations obviously cannot be long-lived. As is seen in this figure, they periodically rearrange with alternation of the mutual positions of the lower-layer vortices after passing through collinear states.

5. The general conditions for the existence of these stationary solutions for an arbitrary momentum value of the system are the following.

5.1. Triangular configuration. From Eqs. (1) and (2), it is easy to derive the condition for the existence of the rectilinear motion of this vortex structure:

$$\frac{1 + 2L|\cos\varphi|K_1(2L|\cos\varphi|)}{\cos^2\varphi} = 4[1 - LK_1(L)] \quad (6)$$

with $L = \gamma l$, where l is the length of the lateral side of the isosceles triangle, as well as the expression for the velocity of this structure in the y direction parallel to the base of the triangle:

$$V = -\frac{\kappa\gamma\sin\varphi}{8\pi L}[1 - LK_1(L)]. \quad (7)$$

Equation (6) can be treated as a dispersion equation relating the length of the triangle lateral side to the angle φ adjacent the base. Equation (6) has a (unique) solution $L(\varphi)$ only in the interval $|\varphi| < \pi/3$; i.e., the triangle cannot be equilateral (more exactly, the limiting value $|\varphi| = \pi/3$ is an asymptotic one as $L \longrightarrow \infty$ and $|V| \longrightarrow 0$).[1] The velocity of the triangular structure coincides with that of a certain hypothetical pair consisting of vortices located in different layers, having intensities -2κ and 2κ, and spaced by the distance equal to the height of the corresponding isosceles triangle. Figure 4a shows the dispersion curve $L(\varphi)$ and $V(\varphi)$ (7). For $\varphi = 0$, we have $V = 0$, and L takes the value $L_0 = 0.8602$ at which the degenerate (to the segment) symmetric three-vortex configuration is stationary. The extremal values of V are attained for $|\varphi| = 0.82\pi/3$ and $L = 1.874$.

5.2. Collinear configuration. We now denote as A and B, respectively, the quantities X_2^1 and X_2^2 that are proportional to the original distances between the upper-layer vortex (for $X_1^1 = 0$) and its partners from the lower layer. From equations of motion (1), (2), we obtain the following conditions for the uniform motion of the entire configuration as a rigid body along the y axis:

$$\frac{A^2 + AB + B^2}{AB(A + B)} = K_1(A) + K_1(B) + K_1(A + B). \quad (8)$$

This equality can also be treated as a dispersion equation relating the geometric parameters of the solutions in the form of the translational collinear configurations. The translational velocity is expressed as

$$V = \frac{\kappa\gamma}{4\pi}\left[\frac{1}{A} - K_1(A) - \frac{1}{B} + K_1(B)\right]. \quad (9)$$

[1] In the homogeneous fluid [10], a similar stationary state is the configuration in the form of an equilateral triangle with an arbitrary side length.

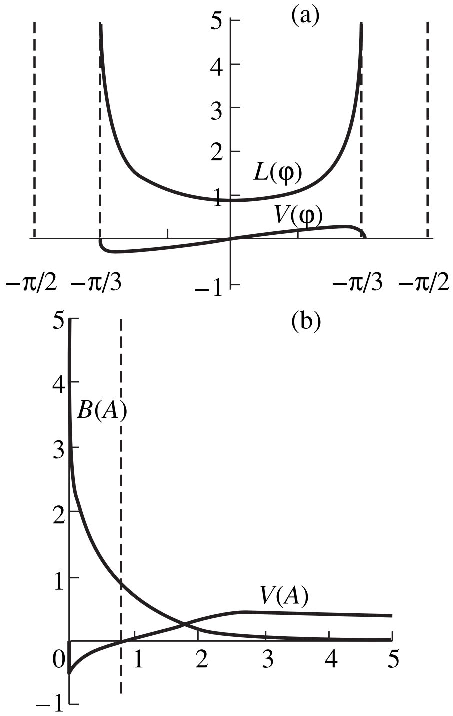

Fig. 4. Geometry parameters characterizing stationary solutions for the (a) triangular and (b) collinear configurations.

Figure 4b demonstrates dispersion curve (8) and vortex-structure velocity (9). In the asymptotic limit as $A \longrightarrow 0$ or $B \longrightarrow 0$, i.e., when the coordinates of a lower-layer vortex coincide with those of the upper-layer vortex, we have, respectively, $B \longrightarrow \infty$ and $A \longrightarrow \infty$. This implies that the second vortex in the lower layer is infinitely far away. The limiting velocity of the configuration also tends to zero but takes extremal values for A/B and $B/A = 0.0075$. The condition $A < B$ ($A > B$) leads to $V < 0$ ($V > 0$). For $A = B$, the velocity reverses its sign. In this case, the conditions $X_2^1 = X_2^2 = L_0$ are satisfied with the same value of L_0, which is observed when the triangular configuration with the symmetric location of the cyclonic vortices degenerates with respect to the upper-layer anticyclonic vortex (see Section 5.1).

6. In conclusion, we emphasize that, in the present study, modes intrinsic to the problem of a system of three vortices in a two-layer rotating fluid with layers of identical thickness values are classified for the case when the total intensity of the system is zero and the lower-layer vortices are equivalent to each other. New stationary solutions are obtained, and general conditions for their existence are found.

ACKNOWLEDGMENTS

We are grateful to V.M. Gryanik, J.B. Flór, V.N. Zyryanov, G.M. Reznik, and Z.I. Kizner for valuable discussions of the results of this study. The work of one of the authors (M.A.S.) was supported by the Russian Foundation for Basic Research (project no. 01-05-64646) and by the Centre National de la Recherche Scientifique, Grenoble, France.

REFERENCES

1. A. V. Borisov and I. S. Mamaev, *Poisson's Structures and Lie Algebras in Hamiltonian Mechanics* (Izd. Dom Udmurtskiĭ Univ., Izhevsk, 1999).
2. V. M. Gryanik, Izv. Akad. Nauk SSSR, Fiz. Atm. Okeana **19**, 227 (1983).
3. V. M. Gryanik, Izv. Akad. Nauk SSSR, Fiz. Atm. Okeana **24**, 1251 (1988).
4. V. V. Kozlov, *General Theory of Vortices* (Izd. Dom Udmurtskiĭ Univ., Izhevsk, 1998).
5. V. V. Meleshko and M. Yu. Konstantinov, *Dynamics of Vortex Structures* (Naukova Dumka, Kiev, 1993).
6. H. Poincaré, *Théorie des turbillions* (Georges Carré, Paris, 1893; Nauchno-Informatsionnyĭ Tsentr: Regulyarnaya i Khaoticheskaya Dinamika, Moscow–Izhevsk, 2000).
7. H. Aref, Phys. Fluids **22**, 393 (1979).
8. X. J. Carton and S. M. Correard, in *Proceedings of International Union of Theoretical and Applied Mechanics, Symposium on Separated Flows and Jets, Lyngby, Denmark, 1997* (Kluwer Acad. Publ., Lyngby, 1997).
9. G. R. Flierl, V. D. Larichev, J. C. McWilliams, and G. M. Reznik, Dyn. Atm. Oceans **5**, 1 (1980).
10. G. J. F. van Heijst, Meccanica **29**, 431 (1994).
11. N. G. Hogg and H. M. Stommel, Proc. R. Soc. London, Ser. A **397**, 1 (1985).
12. B. Legras, R. Santangelo, and R. Benzi, Europhys. Lett. **5**, 37 (1988).
13. C. E. Leith, Phys. Fluids **27**, 1388 (1984).
14. N. J. Rott, Appl. Math. Phys. (ZAMP) **40**, 473 (1989).
15. J. L. Synge, Can. J. Math. **1**, 257 (1949).

Translated by R. Tyapaev